A $SC_{0.28}AL_{0.72}N$ LAMINATED BULK ACOUSTIC WAVE RESONATOR WITH SELF-OVEN-CONTROLLED SWITCHABILITY

Shaurya Dabas, Dicheng Mo, Sushant Rassay, and Roozbeh Tabrizian*
Department of Electrical and Computer Engineering, University of Florida, USA

ABSTRACT

This abstract reports an intrinsically switchable 7.01 GHz thickness-extensional bulk acoustic wave (BAW) scandium-aluminum nitride ($Sc_{0.28}Al_{0.72}N$) resonator with a reduced switching voltage using self-ovenization. The resonator is created from alternative stacking of two $Sc_{0.28}Al_{0.72}N$ layers with three electrode layers, enabling tailorability of transducer polarization across the thickness and based on ferroelectricity. Upon aligning the polarization of the two $Sc_{0.28}Al_{0.72}N$ layers in the same or opposite directions, the electromechanical coupling of the thickness-extensional mode is maximized or nulled, resulting in operation of the resonator in On and Off states, respectively. Besides, the switching voltage is significantly reduced by self-ovenization of the resonator through a DC-biased serpentine-shaped top electrode and due to the temperature-dependent reduction in $Sc_{0.28}Al_{0.72}N$ coercive field. A prototype is demonstrated at 7.01 GHz with a k_t^2 of 6.95% and a loaded Q of 72.2. The intrinsic switchability is successfully demonstrated with and without self-ovenization, using 25kHz triangular pulses with 80.6V and 63.6V amplitude, respectively. The presented results highlight the potential of self-ovenization to reduce the large switching voltage of $Sc_{0.28}Al_{0.72}N$ resonators and filters for configurable RF front-end applications.

KEYWORDS

Intrinsic switchability; ferroelectric; scandium aluminum nitride; Joule heating; ovenization; bulk acoustic wave resonator.

INTRODUCTION

Scandium-aluminum nitride ($Sc_xAl_{1-x}N$) is growingly considered to replace aluminum nitride films that are currently used for creation of radio-frequency acoustic resonators and filters for wireless systems. The significantly larger electromechanical coupling (k_t^2) that only increases with Sc content enables realization of filters with higher bandwidth and lower loss. Further, the newly discovered ferroelectricity in $Sc_xAl_{1-x}N$ provides unprecedented opportunities for realization of intrinsic switchability and tunability without the need for external switches and varactors. This is highly desirable considering the adoption of multi-band RF front-end to accommodate efficient communication in crowded and congested ecosystem of the modern connected world [1,2].

Using polarization tuning for intrinsic switching has been widely explored in acoustic resonators created in perovskite ferroelectric or paraelectric films, such as PZT and BST [3-5]. These materials generally provide a soft ferroelectric behavior, where the polarization, dielectric constant, and piezoelectric coupling can be continuously tuned by application of a DC voltage. This is not the case in $Sc_xAl_{1-x}N$ resonator with hard ferroelectric behavior, where the box-shaped hysteresis loop only allows binary polarization states with similar electromechanical coupling [6]. Targeting the intermediate polarization states through application of DC voltage is also not trivial in $Sc_xAl_{1-x}N$, considering the undesirably close breakdown and coercive fields. Besides, the large coercive field of $Sc_xAl_{1-x}N$, which is nearly two orders of magnitude higher compared to conventional perovskites, results in very large switching and tuning voltages that is hard to provide on chip.

Despite these challenges, a new wave of intrinsically switchable $Sc_xAl_{1-x}N$ BAW and Lamb wave resonators are recently demonstrated, based on tuning polarization through application of low-frequency pulses [7-12]. In these approaches, switching pulses with slightly lower voltage than coercive is applied, to enable "transducer depolarization" through reversing c-axis in a fraction of ferroelectric domains and reducing the net electromechanical coupling by charge cancellation. This approach, however, is not reliable due to the uncertain nature of partial domain switching.

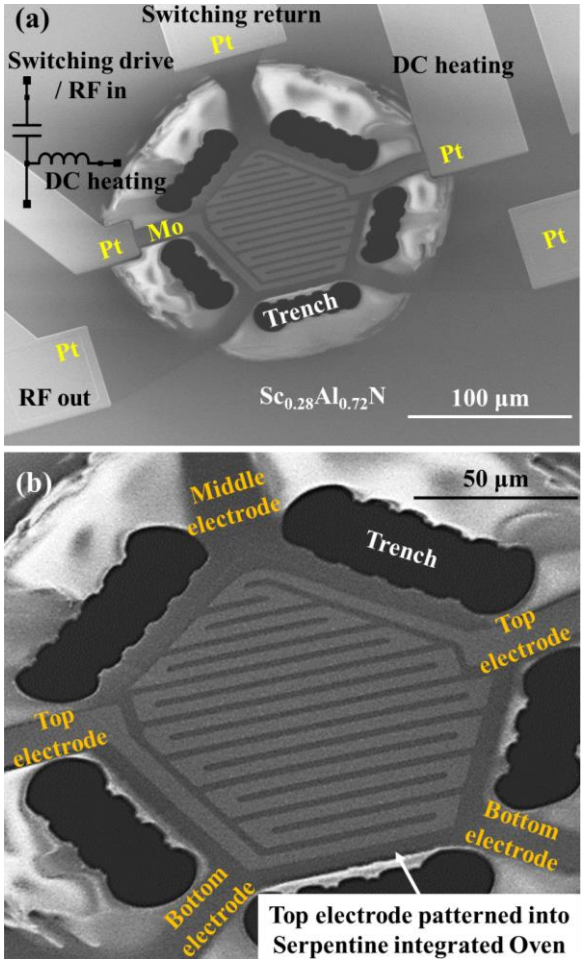

Fig. 1. (a) Top-view SEM image of the intrinsically switchable BAW resonator created in laminated $Sc_{0.28}Al_{0.72}N$ *transducer. (b) Zoomed-in SEM of the top electrode which is patterned to form integrated oven for Joule heating the resonator.*

In this work, for the first time, we demonstrate certain and repeatable switchability in BAW resonator by laminating two $Sc_{0.28}Al_{0.72}N$ layers and controlling their individual polarization. This laminate resonator shown in Fig. 1(a) enables switching of the resonator between On and Off states, upon pulsed poling of the two $Sc_{0.28}Al_{0.72}N$ layers in the same or opposite direction, respectively. Besides, we demonstrate a novel approach for reduction of switching voltage based on self-ovenizing the resonator through Joule heating. Self-ovenization by Joule heating by applying a DC current through the serpentine top electrode (Fig. 1(b)) enables a significant reduction in coercive field and switching voltage.

OPERATION PRINCIPLE

The intrinsically switchable resonator is created from alternative stacking of two $Sc_{0.28}Al_{0.72}N$ layers within three molybdenum (Mo) electrodes. Exciting the fundamental thickness extensional (TE_1) mode in ferroelectric requires alignment of mechanical mode shape, ferroelectric polarization, and applied electric field. Accordingly, upon switching the polarization of the two $Sc_{0.28}Al_{0.72}N$ layers in opposite directions, the net polarization (P) across laminate thickness is reduced to zero, which results in a nulled electromechanical coupling of the TE_1 mode, and the resonator is turned off. Such switching is not achievable in a single-layer BAW resonator, considering the hard ferroelectric behavior of $Sc_xAl_{1-x}N$. This characteristic limits the practical polarization of each ferroelectric domain to either up or down; thus, depolarization approaches used in soft ferroelectric and piezoelectric materials (*e.g.* PZT and BST) is not applicable. Depolarization of $Sc_xAl_{1-x}N$ can be achieved through partial switching of domains using low-frequency pulses with slightly lower value compared to coercive. However, this approach is highly uncertain and achieving repeatable depolarized state is not practical. The comparison of intrinsic switching in single-layer and laminated $Sc_xAl_{1-x}N$ transducer is conceptually shown in Fig. 2. It is evident how the laminated transducer enables deterministic switching based on complete polarization reversal in the bottom $Sc_xAl_{1-x}N$ layer, to oppose the top and null the electromechanical coupling for TE_1 mode.

In this work, the laminated transducer is further equipped with a serpentine-shaped top electrode to enable integrated ovenization of the resonator through application of a DC current and via Joule heating. The integrated heater enables temporary ovenization of the resonator during polarization switching, to benefit from large reduction in coercive field of $Sc_xAl_{1-x}N$ [6]. This facilitates reduction of the resonator switching voltage.

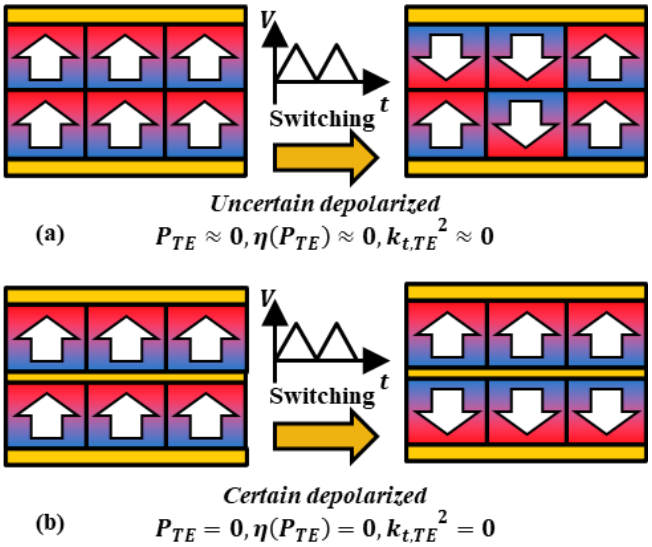

Figure 2. (a) Single-layer resonator switching by depolarizing the ferroelectric film. This is difficult as it requires extremely precise pulse control to pole exactly 50% of crystal domains into the opposite direction. (b) The deterministic switching concept of the presented laminated double-layer resonator, based on complete polarization reversal in one of the layers.

FABRICATION PROCESS

Figure 4 shows a detailed process flow. The laminated resonator is created by sputtering a 50nm bottom Mo electrode atop of a 50nm AlN seed layer. The AlN seed layer helps textured growth of (110) Mo and facilitate crystalline growth of subsequent $Sc_{0.28}Al_{0.72}N$ films in c-axis orientation. Further, the seed layer ensures the suppression of abnormal grains with undesired crystal morphology [13, 14]. After patterning the bottom Mo electrode, 140nm bottom $Sc_{0.28}Al_{0.72}N$ film is sputtered followed by deposition and patterning of 50nm middle Mo electrode. Finally, 140nm of top $Sc_{0.28}Al_{0.72}N$ film is sputtered followed by deposition and patterning of the top 50nm Mo electrode into serpentine heaters. The bottom and middle Mo electrodes are patterned using proximity-exposed photoresist etch-mask and BCl_3 dry-etch recipe to form a highly tapered sidewall profile. This profile is shown in Fig. 3 and is required to ensure crack-free growth of $Sc_{0.28}Al_{0.72}N$ layers.

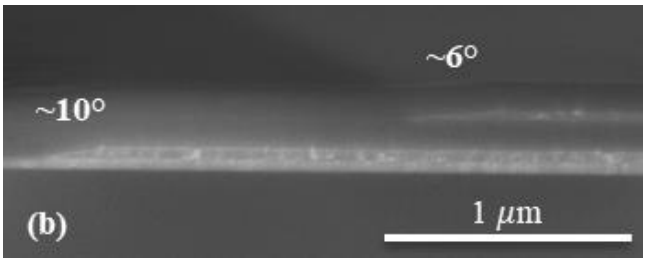

Figure 3. Tapered sidewall of bottom and middle Mo electrodes enables crack-free growth of $Sc_{0.28}Al_{0.72}N$ layers.

After completion of the transducer stack, bottom and middle electrodes are accessed by dry etching of $Sc_{0.28}Al_{0.72}N$ layers using a high-power Cl_2 recipe. A thick platinum (Pt) layer is deposited using liftoff, to serve for low-loss routings and pad. Trenches are then etched to define the geometry of the resonator. Finally, the device is released by etching Si handle-layer from backside via the Bosch process in a DRIE tool. In this step, the AlN seed layer serves as an etch stop to prevent over-etch into the device and its bottom Mo electrode.

CHARACTERIZATION

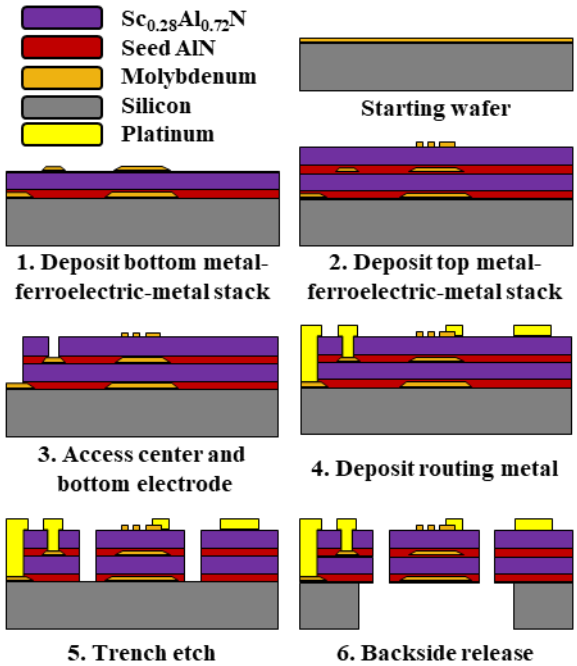

Figure 4. a six-step process flow for laminated bulk acoustic wave resonator with self-oven-controlled switchability.

The laminated $Sc_{0.28}Al_{0.72}N$ BAW resonators are characterized using ferroelectric and RF measurement. The ferroelectric polarization hysteresis and switching behavior of the constituent $Sc_{0.28}Al_{0.72}N$ layers are measured using a Radiant PiezoMEMS ferroelectric tester with DC probes, and the DC heating voltage across the serpentine electrode are applied using Keysight E36105A DC power supply. Besides, the resonator admittance is extracted from the reflectance (S_{11}) measured using Keysight N5222A PNA vector network analyzer (VNA) with GSG probes calibrated using short-open-load-though procedure with CS-5 calibration substrate. All the measurement are conducted on the Semi-Probe PSL4 RF probe station.

Ferroelectric characterization

The polarization hysteresis loop of the 140nm bottom $Sc_{0.28}Al_{0.72}N$ layer is extracted by exciting the film with 84V, 25kHz bipolar triangular pulses. The polarization hysteresis loop is measured under ovenization through application of different DC voltages across the serpentine electrode. Figure 5 shows the measurement setup, highlighting the ovenization voltage application through a bias-tee. Figure 6 shows the measured hysteresis loops for different DC ovenization voltages, highlighting the reduction of coercive field at higher DC voltages, corresponding to increased temperature of the film. This indicates the reduction in the voltage required for switching resonator upon application of the ovenization. It should be noted that the apparent scaling of the loop in y-axis direction upon increased ovenization voltage direction is due to an increased feedthrough current at higher temperatures, rather than any change in remanent polarization of the film.

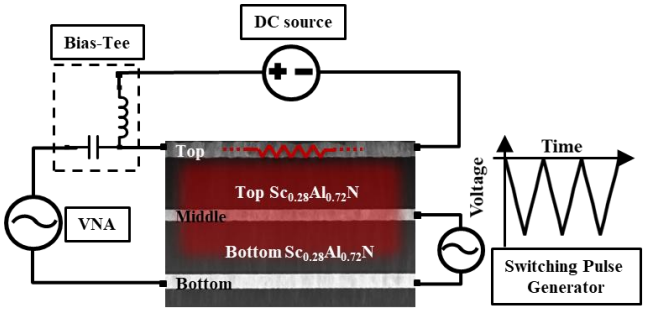

Figure 5. Schematic demonstration of the measurement setup for switching the laminated thickness-extensional resonator. The cross-section of the resonator is shown along with the DC source and pulse generator used for ovenization and polarization switching, respectively.

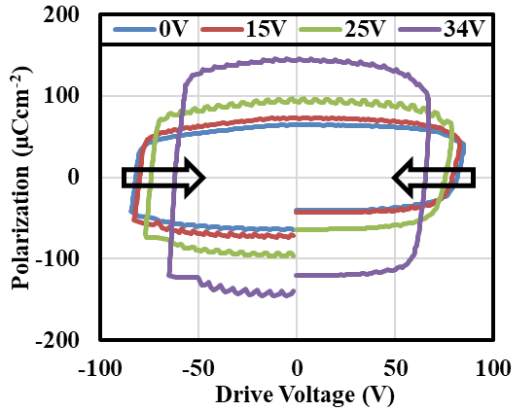

Figure 6: Evolution of the PV loop for bottom $Sc_{0.28}Al_{0.72}N$ layer, for different ovenization voltage (applied across top electrode). The large drop in coercive voltage with increasing ovenization voltage is evident. The apparent increase in polarization is due to increase in leakage current at higher temperatures.

RF characterization

The resonator admittance is extracted from the measured S_{11}, and the ${k_t}^2$ and Q are calculated using [15,16]:

$$ {k_t}^2 = \frac{\pi^2}{8}\left(\frac{{f_p}^2 - {f_s}^2}{{f_s}^2}\right), Q = \frac{f}{2}\left|\frac{\partial \varphi_Y}{\partial f}\right| \quad (1). $$

Here, f_s and f_p are the series and parallel resonant frequency, and φ_Y is admittance phase. Figure 7 here shows the measured admittance of the resonator, as evolving from on-state to off-state upon pulsed switching. A k_t^2 of 6.95% and a Q of 72.2 is measured for the resonator operating in TE_1 BAW mode at 7.01 GHz. The resonator switching is performed by application of two 25kHz 80V monopolar triangular pulses across the bottom $Sc_{0.28}Al_{0.72}N$ layer to induce polarization reversal. The intermediate state, *i.e.*, the admittance after the first pulse, is also shown in Fig. 7. Figure 8 shows the change in switching voltage upon application of DC ovenization voltages, highlighting a ~21% reduction (from 80.5V to 63.6V) once applying 34V DC across the serpentine-shaped top electrode.

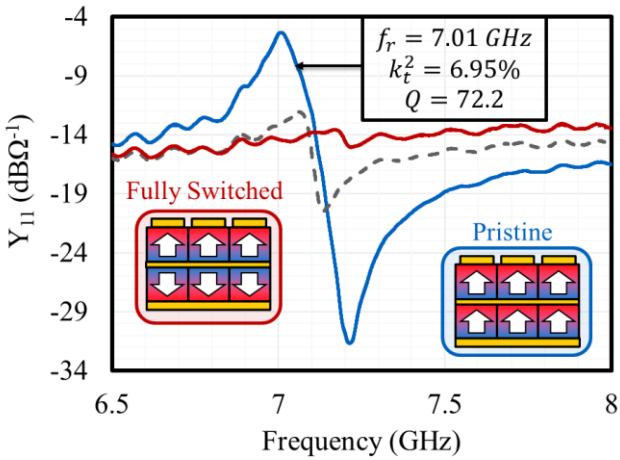

Figure 7: Measured admittance of the laminated ScAlN BAW resonator. The pristine (blue) curve corresponds to the on state; the fully switched (red) admittance response corresponds to the off state by poling the bottom ScAlN layers in opposite direction. The on/off switching resulted in ~10dB isolation. The inset schematics show the polarization direction of ScAlN layers in on and off states.

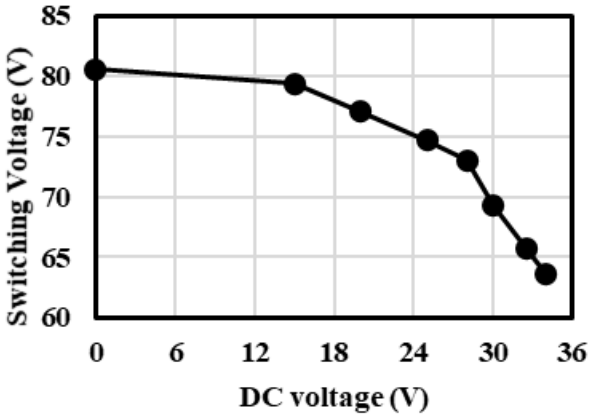

Figure 8: The measured switching voltage for different ovenization voltages. Application of larger ovenization voltage results in significant drop in coercive filed and resonator switching voltage.

CONCLUSION

This paper demonstrates self-oven-controlled intrinsically switchable thickness-extensional BAW $Sc_{0.28}Al_{0.72}N$ resonator operating at 7.01 GHz, with a k_t^2 of 6.95% and Q of 72.2. The intrinsic switchability is realized by using a laminated transducer architecture from alternative stacking of two $Sc_{0.28}Al_{0.72}N$ with three metal electrodes. This configuration enables tailoring transducer polarization across the stack. Once the polarization of the two $Sc_{0.28}Al_{0.72}N$ layers are switched in opposite direction, the resonator is switched off due to the charge cancellation upon excitation of fundamental thickness-extensional mode. The resonator switching voltage is reduced from 80.6V to 63.6V through self-ovenization using a serpentine-shaped top electrode. This concludes the effectiveness of self-ovenization concept for reduction of the large switching voltages in configurable $Sc_{0.28}Al_{0.72}N$ resonators and filters.

ACKNOWLEDGEMENT

The authors would like to thank the University of Florida Nanoscale Research Facility cleanroom staff for fabrication support. This work was supported by Defense Advanced Research Projects Agency (DARPA), Tunable Ferroelectric Nitrides (TUFEN) Program under Grant HR00112090049 and National Science Foundation (NSF) grant ECCS 1752206.

REFERENCE

[1] M. Matthaiou, O. Yurduseven, H. Q. Ngo, D. Morales-Jimenez, S. L. Cotton and V. F. Fusco, "The Road to 6G: Ten Physical Layer Challenges for Communications Engineers", *IEEE Communications Magazine*, 59, 1 (2021).

[2] R. Ruby, "A Snapshot in Time: The Future in Filters for Cell Phones", *IEEE Microwave Magazine*, 16, 7 (2015).

[3] H. Chandrahalim, S. A. Bhave, R. G. Polcawich, J. S. Pulskamp and R. Kaul, "PZT transduced high-overtone width-extensional resonators above 1 GHz", IEEE International Ultrasonics Symposium, Rome, Italy (2009), pp. 2145-2148.

[4] Y. He, B. Bahr, M. Si, P. Ye and D. Weinstein, "A tunable ferroelectric based unreleased RF resonator", *Microsystems & nanoengineering*, 6, 8 (2020).

[5] M. Z. Koohi and A. Mortazawi, "Negative piezoelectric-based electric-field-actuated mode-switchable multilayer ferroelectric FBARs for selective control of harmonic resonances without degrading K_{eff}^2", *IEEE Transactions on Ultrasonics, Ferroelectrics, and Frequency Control*, 67, 9 (2020).

[6] S. Fichtner, N. Wolff, F. Lofink, L. Kienle, and B. Wagner, "AlScN: A III-V semiconductor based ferroelectric", *Journal of Applied Physics*, 125, 11 (2019).

[7] S. Rassay, D. Mo, C. Li, N. Choudhary, C. Forgey and R. Tabrizian, "Intrinsically Switchable Ferroelectric Scandium Aluminum Nitride Lamb-Mode Resonators", *IEEE Electron Device Letters*, 42, 7 (2021).

[8] J. Wang, M. Park, S. Mertin, T. Pensala, F. Ayazi and A. Ansari, "A Film Bulk Acoustic Resonator Based on Ferroelectric Aluminum Scandium Nitride Films", *Journal of Microelectromechanical Systems*, 29, 5 (2020).

[9] S. Dabas, D. Mo, S. Rassay and R. Tabrizian, "Intrinsically Tunable Laminated Ferroelectric Scandium Aluminum Nitride Extensional Resonator Based on Local Polarization Switching", *2022 IEEE 35th International Conference on Micro Electro Mechanical Systems Conference (MEMS)*, Tokyo, Japan (2022), pp. 1050-1053.

[10] S. Rassay, F. Hakim, M. Ramezani and R. Tabrizian, "Acoustically Coupled Wideband RF Filters with Bandwidth Reconfigurability Using Ferroelectric Aluminum Scandium Nitride Film", *2020 IEEE 33rd International Conference on Micro Electro Mechanical Systems (MEMS)*, Vancouver, BC, Canada (2020), pp. 1254-1257.

[11] D. Mo, S. Rassay and R. Tabrizian, "Intrinsically Switchable Ferroelectric Scandium Aluminum Nitride Bulk Acoustic Wave Resonators", *2021 21st International Conference on Solid-State Sensors, Actuators and Microsystems (Transducers)*, Orlando, FL, USA (2021), pp. 317-320.

[12] J. Wang, Y. Zheng and A. Ansari, "Ferroelectric Aluminum Scandium Nitride Thin Film Bulk Acoustic Resonators with Polarization-Dependent Operating States", *Physica Status Solidi (RRL)–Rapid Research Letters*, 15, 5(2021).

[13] V. Felmetsger, M. Mikhov, M. Ramezani and R. Tabrizian, "Sputter Process Optimization for Al0.7Sc0.3N Piezoelectric Films", *2019 IEEE International Ultrasonics Symposium (IUS)*, Glasgow, UK (2019), pp. 2600-2603.

[14] S. Rassay, F. Hakim, C. Li, C. Forgey, N. Choudhary, and R. Tabrizian, "A Segmented-Target Sputtering Process for Growth of Sub-50 nm Ferroelectric Scandium–Aluminum–Nitride Films with Composition and Stress Tuning", *Physica Status Solidi (RRL)–Rapid Research Letters*, 15, 5 (2021).

[15] R. Lu, M. -H. Li, Y. Yang, T. Manzaneque and S. Gong, "Accurate Extraction of Large Electromechanical Coupling in Piezoelectric MEMS Resonators", *Journal of Microelectromechanical Systems*, 28, 2 (2019).

[16] D. A. Feld, R. Parker, R. Ruby, P. Bradley and S. Dong, "After 60 years: A new formula for computing quality factor is warranted", *2008 IEEE Ultrasonics Symposium*, Beijing, China (2008), pp. 431-436.

Contact information

* Shaurya Dabas, tel: +1-407-533-1385; shauryadabas@ufl.edu.